

# A $\pi$ -conjugated, covalent phosphinine framework

Jieyang Huang,<sup>[a, b]</sup> Ján Tarábek,<sup>[b]</sup> Ranjit Kulkarni,<sup>[a, b]</sup> Cui Wang,<sup>[c, f]</sup> Martin Dračinský,<sup>[b]</sup> Glen J. Smales,<sup>[d]</sup> Yu Tian,<sup>[e]</sup> Shijie Ren,<sup>[e]</sup> Brian R. Pauw,<sup>[d]</sup> Ute Resch-Genger,<sup>[c]</sup> and Michael J. Bojdys\*<sup>[a, b]</sup>

**Abstract:** Structural modularity of polymer frameworks is a key advantage of covalent organic polymers, however, only C, N, O, Si and S have found their way into their building blocks so far. Here, we expand the toolbox available to polymer and materials chemists by one additional nonmetal, phosphorus. Starting with a building block that contains a  $\lambda^5$ -phosphinine ( $C_5P$ ) moiety, we evaluate a number of polymerisation protocols, finally obtaining a  $\pi$ -conjugated, covalent phosphinine-based framework (CPF-1) *via* Suzuki-Miyaura coupling. CPF-1 is a weakly porous polymer glass ( $72.4 \text{ m}^2 \text{ g}^{-1} \text{ N}_2$  BET at 77 K) with green fluorescence ( $\lambda_{\text{max}}$  546 nm) and extremely high thermal stability. The polymer catalyzes hydrogen evolution from water under UV and visible light irradiation without the need for additional co-catalyst at a rate of  $33.3 \mu\text{mol h}^{-1} \text{ g}^{-1}$ . Our results demonstrate for the first time the incorporation of the phosphinine motif into a complex polymer framework. Phosphinine-based frameworks show promising electronic and optical properties that might spark future interest in their applications in light-emitting devices and heterogeneous catalysis.

## Introduction

The unique selling point of covalently-linked organic materials – according to the claims of polymer and materials chemists – is their LEGO™-like design. That means, that there is hypothetically an infinite number of organic building blocks (tectons) at our disposal for their fabrication. However, in reality, only a small subset of all available nonmetals has been incorporated into complex polymers, chiefly aromatic carbon. Such materials as porous organic frameworks (POFs),<sup>[1]</sup> conjugated microporous polymers (CMPs)<sup>[2]</sup> and porous aromatic frameworks (PAFs)<sup>[3]</sup>

have been extensively investigated in the fields of gas and energy storage,<sup>[4]</sup> catalysis,<sup>[5]</sup> sensing,<sup>[6]</sup> and in various opto-electronic devices.<sup>[7]</sup> Incorporation of heteroatoms such as nitrogen, sulphur and silicon into the backbone of these polymers yields triazine-based graphitic carbon nitride (TGCN),<sup>[8]</sup> covalent triazine-based frameworks (CTFs),<sup>[9]</sup> sulphur- and nitrogen-containing porous polymers (SNPs),<sup>[10]</sup> and silicate organic frameworks (SiCOFs).<sup>[11]</sup> This has not only led to recent breakthroughs in our understanding of how to construct such extended systems, but it has also uncovered new layers of complexity in material properties. For example, nitrogen-containing CTFs can be used as heterogeneous Periana catalysts and enable low-temperature oxidation of methane to methanol.<sup>[12]</sup> Further, sulphur- and nitrogen-containing polymers feature intimately linked donor-acceptor domains and a narrow bandgap that result in record-breaking performance in photocatalytic water-splitting.<sup>[13]</sup> Despite the confusing three-letter nomenclature in this field, CTFs, CMPs PAFs and SNPs have chiefly in common that they are constructed from covalently-linked  $\pi$ -conjugated building blocks;<sup>[1-3, 9-10]</sup> electron delocalization in polymer framework can improve intriguing properties, especially electric storage and conductivity, bandgap properties, photoluminescence and light harvesting.<sup>[14]</sup> Strategies to expand the properties and applications of  $\pi$ -conjugated frameworks can be broadly divided into two categories; post-synthetic modifications and initial reaction design. Post-synthetic modifications rely on a number of tools such as changes of the polymer topology (*e.g.* by template removal, freeze-drying),<sup>[15]</sup> or various reactions that introduce heteroatoms into the backbone of the network.<sup>[16]</sup> Although post-synthetic modifications enable interesting enhancements of material properties, they are all strongly dependent on initial framework morphologies (compact or open) and suffer from randomness and inhomogeneity in the case of diffusion limited processes. Hence, a more rational pathway to improved,  $\pi$ -conjugated frameworks is the initial design of building blocks (“tectons”).<sup>[1-2, 7, 14, 17]</sup> Design of tectons is the most exciting and promising field for further exploration, as there hitherto only tectons containing the nonmetals C, N, O and S have been explored in any depth.<sup>[9-10, 18]</sup>

All main group elements in first 3 rows of periodic table with four to six valence electrons can form aromatic rings. Lower stability may be the reason why Si and P, which are light elements in the third period of the periodic table and in the same groups as C and N, have never been introduced into  $\pi$ -conjugated frameworks.<sup>[19]</sup> Phosphorus is an outstanding candidate atom to be incorporated into the backbone of materials for a number of reasons: (1) P is electron rich with five valence electrons, like its group V neighbor nitrogen, while it has a larger atomic radius with weaker electronegativity;<sup>[20]</sup> (2) The polarity of C-P bond makes P partially positively charged;<sup>[20b]</sup> (3) phosphorus has a wide range of bonding environments, valence states and coordination numbers to achieve more probable spatial configurations of repeating units;<sup>[20a, 21]</sup> (4) P can increase thermal stability of polymers.<sup>[22]</sup> Moreover, phosphorous-containing molecules are interesting homogeneous catalysts and luminescent dyes.<sup>[23]</sup>

[a] Dr. J. Huang, R. Kulkarni, Dr. M. J. Bojdys  
Department of Chemistry, Humboldt-Universität zu Berlin  
Brook-Taylor-Str. 2, 12489 Berlin (Germany)  
E-mail: m.j.bojdys.02@cantab.net

[b] Dr. J. Huang, Dr. J. Tarábek, R. Kulkarni, Dr. M. Dračinský, Dr. M. J. Bojdys

Institute of Organic Chemistry and Biochemistry of the CAS  
Flemingovo nám. 2, 166 10 Prague (Czech Republic)

[c] C. Wang, Dr. U. Resch-Genger  
Bundesanstalt für Materialforschung und -prüfung (BAM)  
Unter den Eichen 87, 12205 Berlin (Germany)

[d] Dr. G. J. Smales, Dr. B. R. Pauw  
Division Biophotonics, Federal Institute for Materials Research and Testing (BAM)  
Richard-Willstätter-Straße 11, 12489 Berlin (Germany)

[e] Y. Tian, Dr. S. Ren  
College of Polymer Science and Engineering, State Key Laboratory of Polymer Materials Engineering, Sichuan University  
Chengdu 610065 (P. R. China)

[f] C. Wang  
Institute of Chemistry and Biochemistry, Free University of Berlin  
Takustrasse 3, D-14195 Berlin (Germany)

Supporting information and the ORCID identification number(s) for the author(s) of this article can be found under:

<http://dx.doi.org/10.1002/chem.2019xxxxx>

A variety of P-containing polymer frameworks or graphitic materials have been prepared and applied in water treatment, halogen-free flame retardant, transition metal-catalysis, photocatalysis, lithium batteries, gas-selective membranes and biomedical field.<sup>[24]</sup> However, none of these P-containing materials is rationally designed or incorporate phosphorous in an overall aromatic, stable network.<sup>[25]</sup> For example, the P-doped graphitic materials obtained in the past have an entirely random distribution of phosphorus sites.<sup>[20b, 26]</sup> Although the effects of P-doping are real, such statistical functionalizations make it inherently difficult to rationalize any of the observed phenomena.

For the rational design of a  $\pi$ -conjugated, P-containing network, we chose phosphinine – a  $C_5P$  ring, equivalent to pyridine – as the principle building block.<sup>[19b]</sup> Since phosphinine was firstly

atom with a coordination number of 2) and  $\lambda^5$ -phosphinine (a pentavalent phosphorus atom with a coordination number of 4). They show superior fluorescent properties and with applications in organophosphorus chemistry, coordination chemistry, optoelectronics and homogeneous catalysis.<sup>[19b, 25a, 28]</sup> Though a multitude of molecular reactions and their mechanisms are known, to this day, not one polymer based on phosphinines has been achieved.<sup>[25a, 29]</sup> We believe this is because of the high, relative reactivity of the phosphinine P-atom which renders phosphinine incompatible with most polymerisation protocols. For  $\lambda^3$ -phosphinine, the typical electrophilic attack or nucleophilic attack is more preferred at the P-atom.<sup>[30]</sup>  $\lambda^5$ -phosphinine is more stable due to the absence of phosphorus lone pairs, but some strong acids or bases can still attack the P-atom during some

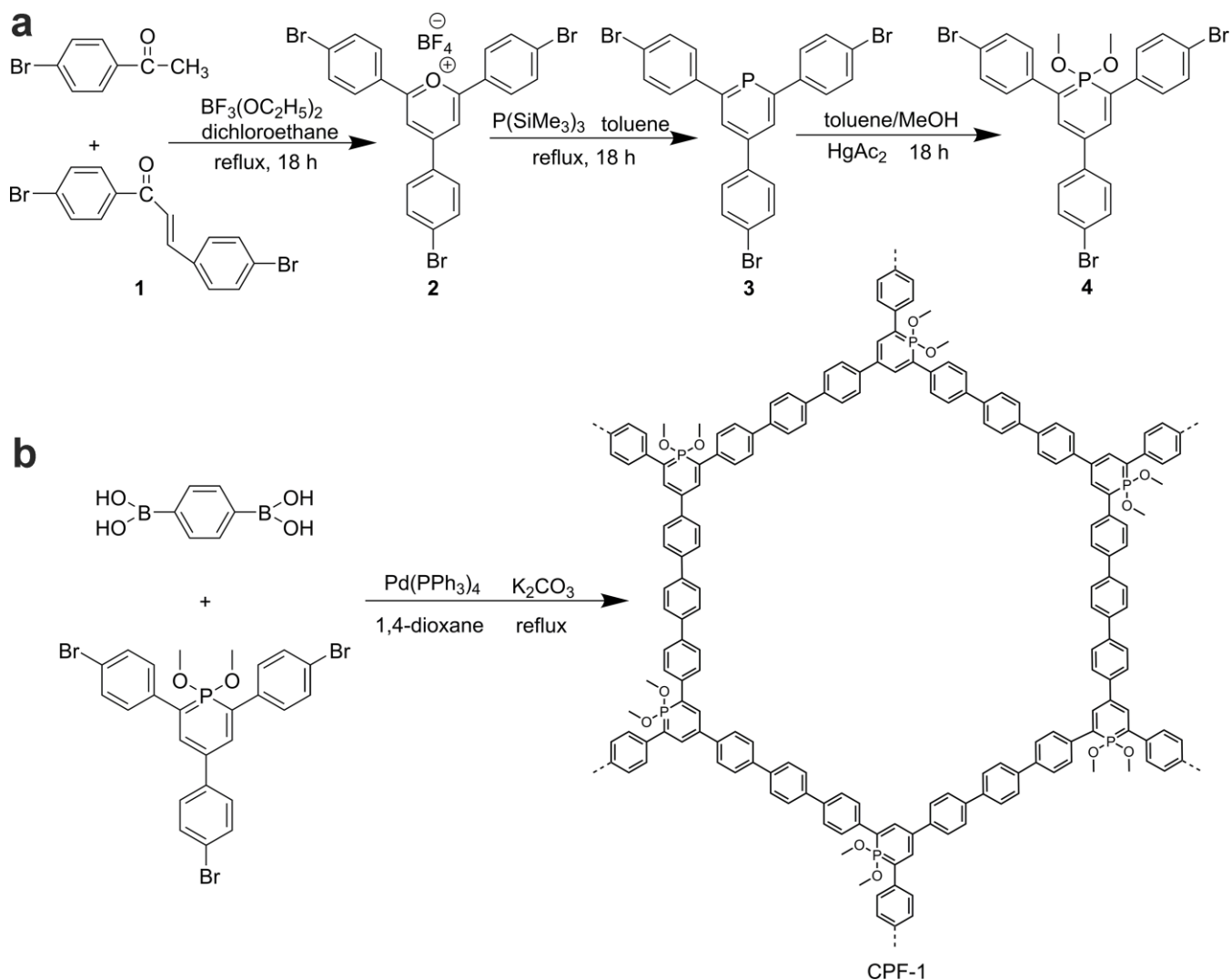


**Figure 1.** (a) Synthetic route for the phosphinine-based tectons **3** and **4**; (b) Suzuki-Miyaura coupling polymerization route of tecton **4** to covalent phosphinine-based framework, CPF-1.

synthesized by Märkl in 1966,<sup>[27]</sup> derivatives of these six-membered  $C_5P$  rings were studied and analyzed for decades. Phosphinines, can contain  $\lambda^3$ -phosphinine (a trivalent phosphorus

polymerisations.<sup>[25a]</sup> Therefore, stable phosphinine-based monomers and mild polymerisation routes need to be carefully chosen to achieve P-containing  $\pi$ -conjugated frameworks.

In this work, we synthesize a stable  $\lambda^5$ -phosphinine-based tecton, and evaluate its stability in a series of common polymerisation protocols. We identify Pd-catalyzed Suzuki-Miyaura coupling as the best approach and thus, obtain the first P-containing fully-aromatic covalent phosphinine-based framework (CPF-1). The structure and properties of CPF-1 were analyzed in detail with a particular focus on optical and electronic factors which are unique to the high content of aromatic phosphorus in the structure.

## Results and Discussion

### Design of phosphinine-based monomers

We design phosphinine-based building blocks with  $C_{2v}$  symmetric bonding axes to achieve fully crosslinked frameworks in analogy to triazine-based frameworks (CTFs).<sup>[9, 31]</sup> Since the phosphinine P-atom influences the reactivity of directly attached substituents considerably,<sup>[29c]</sup> we chose to include aryl spacers on which the polymerizable reactive groups are situated. Combining several reports about synthesis of aryl-halide substituted  $\lambda^3$ -phosphinines,<sup>[32]</sup> and the bromophenyl coupling reaction,<sup>[33]</sup> we obtain 2,4,6-tri(4-bromophenyl)- $\lambda^3$ -phosphinine (**3**) as the principle P-containing tecton. Since previous reports suggest a high reactivity (and hence low stability) of  $\lambda^3$ -phosphinine, we further synthesize the corresponding, protected  $\lambda^5$ -phosphinine compound, 1,1-dimethoxy-2,4,6-tri(4-bromophenyl)- $\lambda^5$ -phosphinine (**4**) as another P-containing tecton.<sup>[25a]</sup> The synthetic routes to monomer **3** and monomer **4** and the subsequent, successful polymerization of tecton **4** to CPF-1 are described in detail in Figure 1.

### Stability of phosphinine-based monomers under common polymerization protocols

We have investigated several conventional, mild polymerization protocols to achieve phosphinine-based polymer networks, *via* reactions of bromophenyl, or its derivative groups of ethynylphenyl and benzonitrile, as shown in Table S1.<sup>[9b, 34]</sup> Since  $\lambda^3$ -phosphinine in particular is very reactive, we evaluate whether the solvent or catalyst attack the ring-phosphorus during the polymerization reaction. After setting up the polymerization of **3** or **4** under conditions described in Table S1 the stability of the phosphinine moiety was checked periodically *via*  $^{31}\text{P}$  NMR spectroscopy. The stabilities of the phosphinine moieties **3** and **4** under different reaction conditions are listed in Table S1 and discussed in more detail in the SI (section S3).

According to Table S1 and S2, the phosphinine ring is attacked and decomposes under most classical polymerization conditions. Especially for the  $\lambda^3$ -phosphinine compound, we were unable to find a compatible polymerization protocol. After  $\lambda^3$ -phosphinine is protected by MeO-groups, the  $\lambda^5$ -phosphinine compound is stable in the presence of  $\text{Pd}(\text{PPh}_3)_4$  and  $\text{K}_2\text{CO}_3$ , but not stable under alkaline conditions.

Even though the options for polymerization are limited, protocols such as Suzuki-Miyaura or coupling remain viable. Therefore, we chose Suzuki-Miyaura coupling in a first attempt to obtain P-containing  $\pi$ -conjugated frameworks, which is described above and in Figure 1b.

### Structure, composition and morphology characterization of CPF-1

Benzene-1,4-diboronic acid, as the most simple, difunctional monomer which is commercially available, was chosen for coupling with tecton **4**, aiming to form  $\pi$ -conjugated frameworks with a classical honeycomb-like structure. Suzuki-Miyaura coupling of tecton **4** yields a brown powder that is insoluble in all solvents tested. We synthesized a corresponding molecular phosphinine compound 1,1-dimethoxy-2,4,6-tri(4-biphenyl)- $\lambda^5$ -phosphinine (PMC) by Suzuki-Miyaura coupling between monomer **4** and phenylboronic acid (Figure S20 in SI) for comparison. The structure of PMC after purification was confirmed by mass,  $^1\text{H}$  NMR and  $^{31}\text{P}$  NMR spectra (Figure S21, S22 and 2c). In  $^{31}\text{P}$  NMR spectrum of PMC, the signal at  $\delta = 68.22$  ppm is characteristic for  $\lambda^5$ -phosphinine.<sup>[28b]</sup>

$^{31}\text{P}$  magic angle spinning (MAS) solid-state NMR (ssNMR) and  $^{13}\text{C}$  cross polarization magic angle spinning (CP-MAS) ssNMR spectra of CPF-1 are shown in Figure 2a and 2b. The two peaks at  $\delta = 62.30$  and 20.30 ppm in the  $^{31}\text{P}$  MAS ssNMR spectrum of CPF-1 are assigned to the ring-P of the  $\lambda^5$ -phosphinine moiety and to  $\text{Ph}_3\text{PO}$ , respectively. Residues of  $\text{Ph}_3\text{PO}$  are a side-product of the decomposition of  $\text{Pd}(\text{PPh}_3)_4$  catalyst (see discussion in Section S4, Figure S23, S24, Section S5, Table S4 and Figure S26).

The  $^{13}\text{C}$  NMR spectrum of PMC has characteristic signals at 115.82 ppm (para-C of P), 94.14/93.24 (ortho-C of P) and 51.85 ppm (C in MeO).<sup>[35]</sup> The other peaks are assigned to phenyl-carbons next to the signals of benzene- $d_6$  (127-128 ppm). The peaks at 119.17 and 117.84 ppm in  $^{13}\text{C}$  NMR spectrum of monomer **4** (Figure S25), which are assigned to halogenated, aromatic carbons (C-Br), cannot be observed in spectrum of PMC nor in the spectrum of CPF-1, also corroborating the high yield of the Suzuki-Miyaura coupling reaction.

$^{13}\text{C}$  CP-MAS ssNMR spectrum of CPF-1 and its assignment are shown in Figure 2b. By comparison with  $^{13}\text{C}$  NMR spectra of PMC and monomer **4**, it is found that the characteristic peaks for  $\lambda^5$ -phosphinine are at 121.80, 88.87, 86.34 and 45.87 ppm, while the signal of halogenated, aromatic carbon (C-Br) cannot be detected.

The combustion elemental analysis (EA) and inductively coupled plasma - optical emission spectrometry (ICP-OES) results reveal that the contents of Pd (0.19 wt%), Br (1.32 wt%) and B (0.01 wt%) are quite low in CPF-1, and the mass ratio of P:H = 1.176 matches with the calculated ratio of 1.178 accurately (Section S5 and Table S3). Further, the ICP-OES results show a mass ratio of C:P in as-received polymer sample of 12.96 which is close to the theoretical value of 13.20 for perfect CPF-1. The low content of Pd, Br and B in particular suggests that only few unreacted end-groups remain after the polymerization and purification steps, and that the observed residuals are trapped within the polymer matrix rather than regularly built into the framework. The FTIR spectra of monomer **4**, PMC, and CPF-1 are shown in Figure 3a. The bands ranging from 2930 to 2830  $\text{cm}^{-1}$  are assigned to C-H stretching vibrations of MeO,<sup>[36]</sup> and the bands between 1005 and 1015  $\text{cm}^{-1}$  are assigned to C-O / P-O

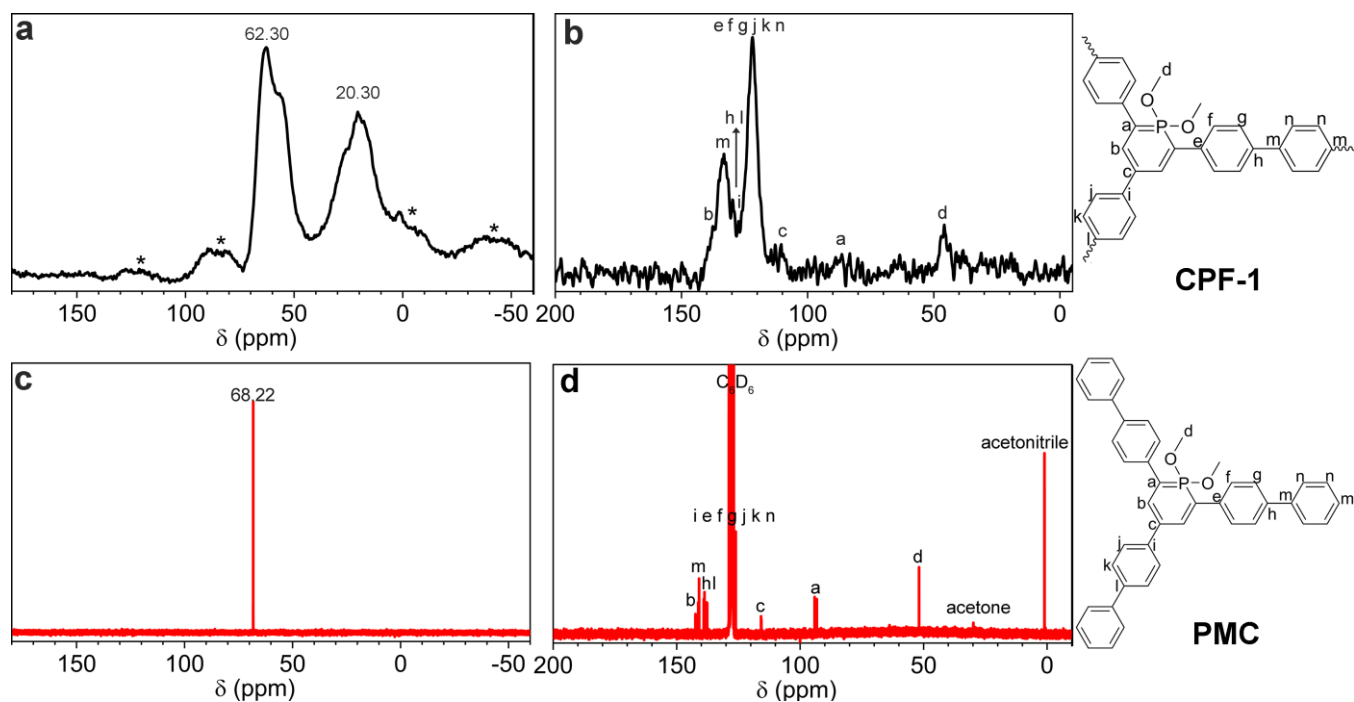


**Figure 2.** (a)  $^{31}\text{P}$  magic angle spinning (MAS) solid-state NMR (ssNMR) spectrum of CPF-1; (b)  $^{13}\text{C}$  CP-MAS ssNMR spectrum of CPF-1; (c)  $^{31}\text{P}$ -NMR spectrum of PMC in benzene- $d_6$ ; (d)  $^{13}\text{C}$  NMR spectrum of PMC in benzene- $d_6$ .

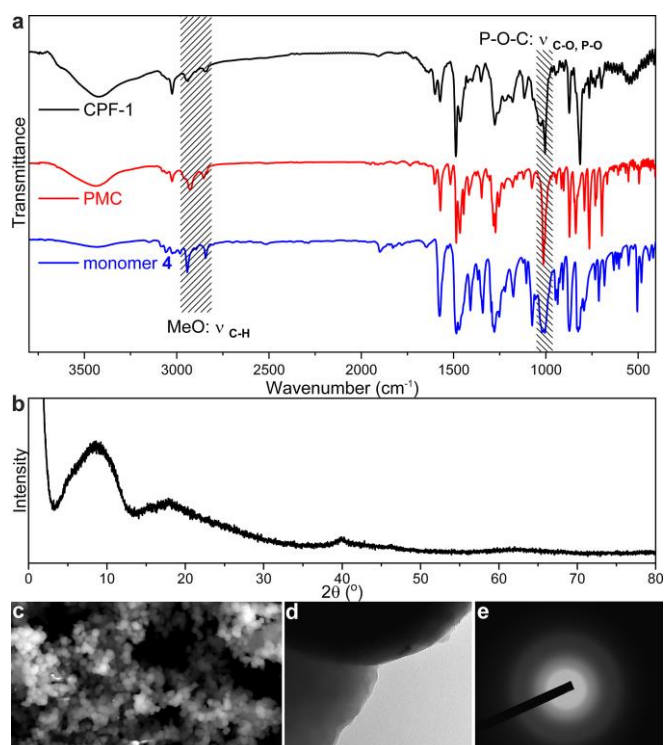


**Figure 3.** (a) FTIR spectra of monomer 4, PMC and CPF-1; (b) PXRD pattern of CPF-1; Electron microscopic investigation of CPF-1: (c) SEM image; (d) TEM image; (e) SAED image.

stretching vibrations of the  $\lambda^5$ -phosphinine (P-O-C).<sup>[37]</sup> These absorption bands appear in all FTIR spectra including the  $\lambda^5$ -phosphinine containing CPF-1 structure.

The powder X-ray diffraction (PXRD) patterns of CPF-1 in Figure 3b shows only a glassy polymer profile, which result is consistent with previous reports of amorphous polymer networks polymerized by Suzuki-Miyaura coupling.<sup>[38]</sup> Transmission electron microscopy (TEM) images and corresponding selected area diffraction (SAED) patterns (Figure 3d and 4e) corroborate amorphous, “cauliflower”-like aggregates with sizes ranging from 0.7 to 1.5  $\mu\text{m}$  with no discernible internal structure, which says two-fold: (1) the “cauliflower”-like aggregates of CPF-1 are indicative for point-nucleation growth, and (2) residual inorganics are dispersed in atomic (rather than macroscopic) aggregates throughout the polymer network.<sup>[9, 31]</sup> SEM analysis (Figure 3c) indicates, Energy-dispersive X-ray (EDX) results (Figure S27 and Table S5) match with the composition data obtained by EA/ICP-OES.

A nitrogen sorption isotherm obtained at 77 K for CPF-1 is seen in Figure S28a, revealing only a weak porosity nature by Brunauer–Emmett–Teller (BET) analysis with a surface area of 72.4  $\text{m}^2 \text{g}^{-1}$ . The surface area of CPF-1 is comparable to structurally analogous, carbon-only conjugated microporous polymers (CMPs).<sup>[38]</sup> NL-DFT pore size distribution analysis shows predominantly pore sizes ranging between 2 to 9 nm (Figure S28b). These pores are also evident by analysis of small angle X-ray scattering (SAXS) data patterns (Figure S29). This data suggests that there are some pores with average radii of 3.156 nm ranging from 1 to 5 nm – much smaller than any of the

particles observed in SEM surveys. Compared with the BET pore size distribution results, the SAXS confirms the presence of micropores. Thermogravimetric analysis (TGA) data shows that CPF-1 is stable up to 350 °C under air and up to 700 °C under nitrogen; in fact, under non-oxidative conditions up to 67% of the mass are retained even at 1000 °C (Figure S30). This is an extraordinarily high thermal and oxidative stability outperforming any of the S- and N-containing polymer frameworks.<sup>[9-10]</sup>

The comprehensive structure characterization of CPF-1, as well as monomer **4** and PMC, demonstrates that a  $\pi$ -conjugated

and stable phosphinine-based framework was successfully prepared, although some catalyst residues remain trapped in the pore structure.

#### Electronic and optical properties of CPF-1

We find that although CPF-1 is  $\pi$ -conjugated, it is not very conductive in macroscopic, pressed-pellet form with conductivity values of  $1.16 \times 10^{-12} \text{ S cm}^{-1}$  (see Section S6). Hence, any new, electronic effects will be found on a local, microscopic level. We see from  $^{13}\text{C}$  CP-MAS ssNMR spectroscopy that CPF-1 has a relatively low signal-to-noise ratio even at increased MAS rates

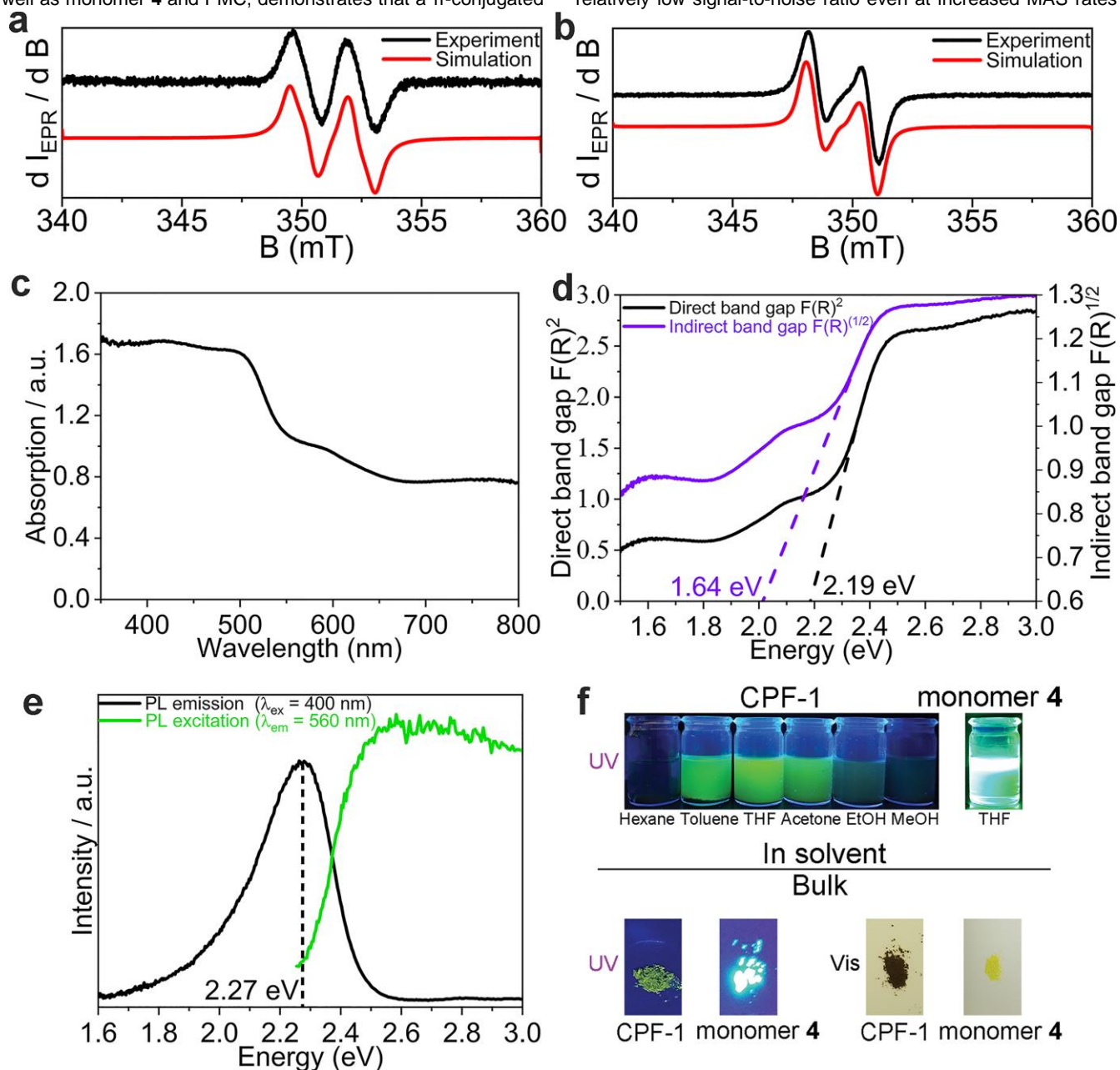


**Figure 4.** EPR spectra of the polycrystalline (powder) samples of (a) monomer **4** and (b) CPF-1 together with simulations of their corresponding radical cation; (c, d) Solid-state UV-vis diffuse-reflectance spectrum of CPF-1; (e) solid-state photoluminescence emission spectrum ( $\lambda_{\text{exc}} = 400 \text{ nm}$ ) and solid-state photoluminescence excitation spectrum ( $\lambda_{\text{em}} = 560 \text{ nm}$ ) of CPF-1; (f) Images of CPF-1 dispersed in various solvents and monomer **4** illumination with UV and visible light.

up to a maximum of 20 kHz, long contact times ( $\tau = 10$  ms) and acquisition times (34.4 ms).  $\lambda^5$ -phosphinine can lose an electron and be oxidized to a radical cation at a lower oxidation potential than the  $\lambda^3$ -phosphinine.<sup>[39]</sup> We probe this by electron paramagnetic resonance (EPR) spectroscopy of monomer **4** and CPF-1. Relevant DFT computations and simulations of EPR spectra for the  $\lambda^5$ -phosphinine radical cation are discussed in Section S6. EPR spectra of paramagnetic monomer **4** and polymer CPF-1 are shown in Figure 4a and 4b together with the simulations of their corresponding radical cation. Both spectra display rhombic symmetry (simulation parameters are summarized in Table S6) showing that radical cationic centers within the polymer as well as within monomer do not possess a well-defined symmetry of the paramagnetic centers. DFT calculation results indicate that maximum electron density is indeed situated on the P-atom ring (see Table S6 and S7 for hyperfine coupling constants and Table S8 for spin population). Taking into account the DFT calculations, simulation of the EPR spectra and DFT computed NBO spin population analysis (Section S6 and Table S8), the EPR spectra confirm that the highest spin density is localized on the central phosphinine moiety for both the tecton **4** and CPF-1. The results match some reports which state that there are radicals localized on the central  $\lambda^5$ -phosphinine moiety.<sup>[39-40]</sup> The radicals remain localized on the ring-phosphorus even after formation of the CPF-1 network, leading to relative broad ssNMR signals with low signal-to-noise ratio. Furthermore, EPR results show that the Suzuki-Miyaura coupling reaction does not change the environment of the  $\lambda^5$ -phosphinine moieties.

According to diffuse reflectance UV-vis spectroscopy, CPF-1 has a discernible absorption edge at around 620 nm (Figure 4c). According to the Kubelka-Munk function this equates to a direct optical band gap of 2.19 eV and an indirect optical band gap of 1.64 eV (Figure 4d). Photoluminescence (PL) spectroscopy of CPF-1 shows one prominent peak observed at excitation transition energy of 2.27 eV, corresponding to a wavelength of 546 nm and green fluorescence (Figure 4e). Figure 4f shows the color of CPF-1 and tecton **4** under visible light and under UV light ( $\lambda_{\text{exc}} = 365$  nm). Because of the electronic interactions between conjugated polymer chains, the fluorescence efficiency of CPF-1 decreases dramatically.<sup>[38]</sup> When CPF-1 is dispersed in organic solvents, especially in THF, it shows again green fluorescence under UV light illumination ( $\lambda_{\text{exc}} = 365$  nm), while monomer **4** shows extraordinarily intense green fluorescence.<sup>[28a]</sup>

Under 365 nm UV light illumination the absolutely measured quantum yield (QY) of monomer **4** is 43.2% (at 78.8% absorption) in the solid-state (ss). CPF-1 only has a QY in the solid state of less than 0.01% (at 81.9% absorption). Dispersed in THF, CPF-1 reveals a QY of 19.0% (at 54.3% absorption), while the QY of tecton **4** is 81.9% (at 28.2% absorption) (Figure S33). Hence, the fluorescence of CPF-1 is a consequence of the incorporation of the  $\lambda^5$ -phosphinine moiety into the polymer backbone. This fluorescence is diminished in the solid state by  $\pi$ - $\pi$  stacking induced quenching, as observed in other  $\pi$ -conjugated, layered polymer systems.<sup>[28a, 41]</sup>

Finally, we tried to utilize CPF-1 for some common catalytic applications such as aerobic oxidation of benzyl alcohol and

photocatalytic hydrogen evolution. For aerobic oxidation experiments, we found that CPF-1 is unable to activate the aerobic oxidation of benzyl alcohol in acetonitrile at 80 °C even after 120 h (Section S7). Similarly, photocatalytic hydrogen evolution under visible light (wavelength 380 to 780 nm) with triethanolamine as the sacrificial agent and 3wt% of Pt co-catalyst yields hydrogen evolution rates lower than  $1 \mu\text{mol h}^{-1} \text{g}^{-1}$ , below the detection limit. Hydrogen evolution under UV and visible light (300 to 2500 nm) is shown in Figure S34. Here, the hydrogen evolution rate of  $29.3 \mu\text{mol h}^{-1} \text{g}^{-1}$  is reached using 3 wt% of Pt co-catalyst. Hydrogen evolution rates stayed roughly constant at  $33.3 \mu\text{mol h}^{-1} \text{g}^{-1}$  when no Pt co-catalyst was added. We assume that residual palladium from the network-forming reaction (0.19 wt% by ICP-OES; Table S3) acts as a co-catalyst in this case.

## Conclusions

In summary, we have synthesized an extended,  $\pi$ -conjugated, covalent phosphinine-based framework (CPF-1), and we addressed two gaps in research: (1) since phosphinine was first synthesized in 1966, we have achieved for the first-time a successful incorporation of the six-membered phosphinine ring into a polymer *via* the Suzuki-Miyamura protocol; (2) we have successfully expanded the family of potential nonmetal-containing tectons available for the rational design of  $\pi$ -conjugated frameworks to C, N, O, S and now P. Two new Br-functionalized monomers containing  $\lambda^3$ -phosphinine and  $\lambda^5$ -phosphinine were obtained in the process and evaluated as building blocks in conventional polymerization protocols. Suzuki-Miyaura coupling was chosen as a conservative polymerization route with no side-reactions on the central P-atom of the  $\lambda^5$ -phosphinine tecton.

We found CPF-1 not only shows remarkable thermal stability (under inert atmosphere) but also retains the green fluorescence of its phosphinine building blocks, guiding towards potential application of CPF-1 as OLEDs. As this is a first step in the investigation of the phosphinine-based polymers, it becomes clear that highly-efficient catalysis, and potential electronic applications will require a reliable preparation protocol of  $\lambda^3$ -phosphinine based polymers in the future.<sup>[42]</sup>

## Experimental Section

**Synthesis of phosphinine-based precursors:** The synthesis of the precursor materials 1,3-Bis(4-bromophenyl)prop-2-en-1-one (**1**) and 2,4,6-tri(4-bromophenyl)pyrylium tetrafluoroborate (**2**) is given in the Supporting Information (Section S1).

**Synthesis of 2,4,6-tri(4-bromophenyl)- $\lambda^3$ -phosphinine (**3**):** The preparation procedure is a modified method based on previous reports for phosphinine compounds.<sup>[28b, 32]</sup> Compound **2** (5.21 g, 8.20 mmol) and 40 mL anhydrous toluene were added to a 100 mL one-neck flask under inert atmosphere in a glovebox.  $\text{P}(\text{SiMe}_3)_3$  (2.06 g, 8.20 mmol) was added dropwise to the flask under continuous stirring. The flask was connected to argon atmosphere on a Schlenk line, and the mixture was stirred and refluxed for 18 h. After volatiles were removed under vacuum, the residue

was purified by column chromatography on silica gel (eluent hexane/CH<sub>2</sub>Cl<sub>2</sub> = 9/1) to give 3.10 g (5.52 mmol for C<sub>23</sub>H<sub>14</sub>Br<sub>3</sub>P, 67.3% yield) of 2,4,6-tri(4-bromophenyl)-λ<sup>3</sup>-phosphinine (**3**) as a white solid. <sup>1</sup>H NMR (400 MHz, (CD<sub>3</sub>)<sub>2</sub>CO): 8.63 (2H, d, *J* = 6.0 Hz), 7.91-7.86 (2H, m), 7.85-7.78 (4H, m), 7.78-7.70 (6H, m) (see Figure S4). <sup>31</sup>P NMR (162 MHz, (CD<sub>3</sub>)<sub>2</sub>CO): 186.27 (see Figure S5). Note: 2,4,6-tri(4-bromophenyl)-λ<sup>3</sup>-phosphinine is not stable in CDCl<sub>3</sub>.

**Synthesis of 1,1-dimethoxy-2,4,6-tri(4-bromophenyl)-λ<sup>5</sup>-phosphinine (**4**):** The preparation procedure was adapted from K. Dimruth et al.<sup>[43]</sup> Compound **3** (3.10 g, 5.52 mmol), mercury(II) acetate (1.76 g, 5.53 mmol), 150 mL anhydrous MeOH and 150 mL anhydrous toluene were stirred under argon atmosphere at room temperature for 12 h. After the liquid was removed under vacuum, the residue was purified by column chromatography on silica gel (eluent hexane/CH<sub>2</sub>Cl<sub>2</sub> = 8/2) to give 2.40 g (3.85 mmol) crude product. The crude product was recrystallized from acetonitrile overnight to form green/yellow product 1,1-dimethoxy-2,4,6-tri(4-bromophenyl)-λ<sup>5</sup>-phosphinine (**4**) 2.06 g (3.31 mmol for C<sub>25</sub>H<sub>20</sub>Br<sub>3</sub>O<sub>2</sub>P, 60.0% yield). <sup>1</sup>H NMR (400 MHz, (CD<sub>3</sub>)<sub>2</sub>CO): 8.00 (2H, d, *J* = 36.6 Hz), 7.64-7.57 (8H, m), 7.57-7.44 (4H, m), 3.50 (6H, d, *J* = 13.8 Hz) (see Figure S6). <sup>31</sup>P NMR (162 MHz, (CD<sub>3</sub>)<sub>2</sub>CO): 66.44 (see Figure S7). MS (APCI): calculated for [C<sub>25</sub>H<sub>21</sub>O<sub>2</sub>Br<sub>3</sub>P] 620.88238, found 620.88248 (see Figure S8).

**Synthesis of π-conjugated covalent phosphinine-based framework (CPF-1):** Polymerization was achieved with a palladium-catalyzed Suzuki-Miyaura coupling process.<sup>[34c, 38, 44]</sup> Monomer **4** (732 mg, 1.17 mmol), benzene-1,4-diboronic acid (292 mg, 1.76 mmol) and Pd(PPh<sub>3</sub>)<sub>4</sub> catalyst (102 mg, 0.0880 mmol) were added to a 250 mL three-neck flask and purged under argon. 80 mL 1,4-dioxane was degassed by argon bubbling for 20 min and then added to the flask under continuous stirring. 12.5 mL aqueous K<sub>2</sub>CO<sub>3</sub> solution were degassed by argon bubbling for 20 min and then added to the flask. The mixture was degassed by argon bubbling for a further 30 min, and subsequently stirred and refluxed under argon atmosphere for 80 h. The precipitate was collected by filtration and washed with THF, CHCl<sub>3</sub>, hot water and MeOH, and further purification was carried out by Soxhlet extraction for two days using THF and MeOH. The product was washed with 200 mL water at 90 °C three times to remove K<sub>2</sub>CO<sub>3</sub>, and the brown powder was finally dried at 120 °C for 12 h in vacuum to afford CPF-1 0.4558 g (0.458 mmol for C<sub>68</sub>H<sub>52</sub>O<sub>4</sub>P<sub>2</sub>, 78.3% yield). Calculated for CPF-1: C, 82.07; H, 5.28; O, 6.43; P, 6.22. Found: C, 73.47; H, 4.82; P, 5.67; K, 0.3; Pd, 0.19; Br, 1.32; B, 0.01.

## AUTHOR INFORMATION

### Corresponding Author

\*E-mail: m.j.bojdys.02@cantab.net

### ORCID

Dr. Jieyang Huang 0000-0001-8169-7054

Dr. Ján Tarábek 0000-0003-0116-3824

Ranjit Kulkarni 0000-0002-8251-1407

Cui Wang 0000-0002-7446-6685

Dr. Martin Dračinský 0000 - 0002 - 4495 - 0070

Dr. Glen J. Smales 0000-0002-8654-9867

Yu Tian 0000-0002-7888-1421

Dr. Shijie Ren 0000-0002-7562-8666

Dr. Brian R. Pauw 0000-0002-8605-838X

Dr. Ute Resch-Genger 0000-0002-0944-1115

Dr. Michael J. Bojdys 0000-0002-2592-4168

## Acknowledgements

J.H. carried out the synthetic experiments, analyzed the data and wrote the paper. J.T. carried out the EPR measurements and analysis, EPR simulation and DFT computation. R.K. carried out the BET measurements and analysis, and the aerobic oxidation experiments. C.W. and U.R. carried out the optical properties measurements and analysis. M.D. carried out the ss-NMR measurements and NMR analysis. G.J.S. and B.R.P. carried out the SAXS-WAXS measurements and analysis. Y.T. and S.R. carried out the hydrogen evolution experiments and analysis. M.J.B. conceived the project and wrote the paper.

We thank Barbora Balcarova for N<sub>2</sub> sorption measurements, Dr. Lucie Bednářová for FTIR spectroscopy, Dr. Radek Pohl for NMR measurements, Romana Hadravová for TEM measurements, Stanislava Matějková for EA/ICP-OES, Dr. Yu Noda for conductivity measurements, Yi Xiong for graphical abstract design, Pengbo Lyu and Prof. Dr. Petr Nachtigall for DFT calculated EPR parameters. M.J.B. thanks the European Research Council (ERC) for funding under the Starting Grant Scheme (BEGMAT-678462).

## Conflict of interest

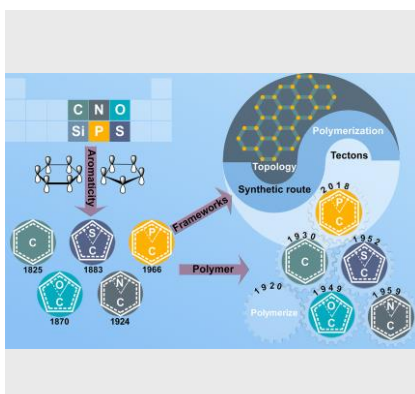
The authors declare no conflict of interest.

**Keywords:** phosphinine • π-conjugated frameworks • Suzuki-Miyaura coupling • polymers • fluorescence

- [1] X. Zou, H. Ren, G. Zhu, *Chem. Commun.* **2013**, 49, 3925-3936.
- [2] R. Dawson, A. Trewin, in *Porous Polymers*, **2015**, pp. 155-185.
- [3] T. Ben, S. Qiu, *CrystEngComm* **2013**, 15, 17-26.
- [4] W. Lu, D. Yuan, D. Zhao, C. I. Schilling, O. Plietzsch, T. Muller, S. Bräse, J. Guenther, J. Blümel, R. Krishna, *Chem. Mater.* **2010**, 22, 5964-5972.
- [5] J. X. Jiang, F. Su, A. Trewin, C. D. Wood, N. L. Campbell, H. Niu, C. Dickinson, A. Y. Ganin, M. J. Rosseinsky, Y. Z. Khimyak, *Angew. Chem. Int. Ed.* **2007**, 46, 8574-8578.
- [6] X. Liu, Y. Xu, D. Jiang, *J. Am. Chem. Soc.* **2012**, 134, 8738-8741.
- [7] Y. Xu, S. Jin, H. Xu, A. Nagai, D. Jiang, *Chem. Soc. Rev.* **2013**, 42, 8012-8031.
- [8] G. Algara - Siller, N. Severin, S. Y. Chong, T. Björkman, R. G. Palgrave, A. Laybourn, M. Antonietti, Y. Z. Khimyak, A. V. Krasheninnikov, J. P. Rabe, *Angew. Chem.* **2014**, 126, 7580-7585.

- [9] a) P. Katekomol, J. r. m. Roeser, M. Bojdys, J. Weber, A. Thomas, *Chem. Mater.* **2013**, *25*, 1542-1548; b) S. Ren, M. J. Bojdys, R. Dawson, A. Laybourn, Y. Z. Khimyak, D. J. Adams, A. I. Cooper, *Adv. Mater.* **2012**, *24*, 2357-2361; c) M. J. Bojdys, J. Jeromenok, A. Thomas, M. Antonietti, *Adv. Mater.* **2010**, *22*, 2202-2205.
- [10] a) D. Schwarz, A. Acharja, A. Ichangi, P. Lyu, M. V. Opanasenko, F. R. Goßler, T. A. König, J. Čejka, P. Nachtigall, A. Thomas, *Chem. Eur. J.* **2018**, *24*, 11916-11921; b) D. Schwarz, Y. S. Kochergin, A. Acharjya, A. Ichangi, M. V. Opanasenko, J. Čejka, U. Lappan, P. Arki, J. He, J. Schmidt, *Chem. Eur. J.* **2017**, *23*, 13023-13027.
- [11] J. Roeser, D. Prill, M. J. Bojdys, P. Fayon, A. Trewin, A. N. Fitch, M. U. Schmidt, A. Thomas, *Nat. Chem.* **2017**, *9*, 977.
- [12] R. Palkovits, M. Antonietti, P. Kuhn, A. Thomas, F. Schüth, *Angew. Chem. Int. Ed.* **2009**, *48*, 6909-6912.
- [13] Y. S. Kochergin, D. Schwarz, A. Acharjya, A. Ichangi, R. Kulkarni, P. Eliášová, J. Vacek, J. Schmidt, A. Thomas, M. J. Bojdys, *Angew. Chem. Int. Ed.* **2018**, *57*, 14188-14192.
- [14] A. I. Cooper, *Adv. Mater.* **2009**, *21*, 1291-1295.
- [15] a) A. Thomas, *Angew. Chem. Int. Ed.* **2010**, *49*, 8328-8344; b) Y. Xu, Z. Lin, X. Huang, Y. Wang, Y. Huang, X. Duan, *Adv. Mater.* **2013**, *25*, 5779-5784.
- [16] W. Lu, D. Yuan, J. Sculley, D. Zhao, R. Krishna, H.-C. Zhou, *J. Am. Chem. Soc.* **2011**, *133*, 18126-18129.
- [17] M. J. Bojdys, *Macromol. Chem. Phys.* **2016**, *217*, 232-241.
- [18] a) S. B. Alahakoon, C. M. Thompson, G. Occhialini, R. A. Smaldone, *ChemSusChem* **2017**, *10*, 2116-2129; b) N. Huang, P. Wang, D. Jiang, *Nat. Rev. Mater.* **2016**, *1*, 16068; c) U. Díaz, A. Corma, *Coord. Chem. Rev.* **2016**, *311*, 85-124.
- [19] a) K. Abersfelder, A. J. White, H. S. Rzepa, D. Scheschke, *Science* **2010**, *327*, 564-566; b) P. Le Floch, in *Phosphorous Heterocycles I*, Springer, **2008**, pp. 147-184.
- [20] a) S. Zhang, X. Zhao, B. Li, C. Bai, Y. Li, L. Wang, R. Wen, M. Zhang, L. Ma, S. Li, *J. Hazard. Mater.* **2016**, *314*, 95-104; b) M. A. Patel, F. Luo, M. R. Khoshi, E. Rabie, Q. Zhang, C. R. Flach, R. Mendelsohn, E. Garfunkel, M. Szostak, H. He, *ACS nano* **2016**, *10*, 2305-2315.
- [21] B. W. Rawe, D. P. Gates, *Angew. Chem. Int. Ed.* **2015**, *54*, 11438-11442.
- [22] R.-J. Jeng, S.-M. Shau, J.-J. Lin, W.-C. Su, Y.-S. Chiu, *Eur. Polym. J.* **2002**, *38*, 683-693.
- [23] a) P. Le Floch, *Coord. Chem. Rev.* **2006**, *250*, 627-681; b) X. D. Jiang, J. Zhao, D. Xi, H. Yu, J. Guan, S. Li, C. L. Sun, L. J. Xiao, *Chem. Eur. J.* **2015**, *21*, 6079-6082.
- [24] a) P. Mohanty, L. D. Kull, K. Landskron, *Nat. Commun.* **2011**, *2*, 401; b) Z. Hu, Z. Shen, C. Y. Jimmy, *Green Chem.* **2017**, *19*, 588-613; c) L. Xu, R. Hu, B. Z. Tang, *Macromolecules* **2017**, *50*, 6043-6053; d) S. Popa, S. Iliescu, G. Iliu, N. Plesu, A. Popa, A. Visa, L. Macarie, *Eur. Polym. J.* **2017**, *94*, 286-298.
- [25] a) P. Le Floch, in *Phosphorus-Carbon Heterocyclic Chemistry*, Elsevier, **2001**, pp. 485-533; b) C. S. Lin, J. Li, C. W. Liu, *Chin. J. Chem.* **1997**, *15*, 289-295.
- [26] a) H. Zhang, X. Li, D. Zhang, L. Zhang, M. Kapilashrami, T. Sun, P.-A. Glans, J. Zhu, J. Zhong, Z. Hu, *Carbon* **2016**, *103*, 480-487; b) Y. Zhou, L. Zhang, J. Liu, X. Fan, B. Wang, M. Wang, W. Ren, J. Wang, M. Li, J. Shi, *J. Mater. Chem. A* **2015**, *3*, 3862-3867; c) L. Jing, R. Zhu, D. L. Phillips, J. C. Yu, *Adv. Funct. Mater.* **2017**, *27*, 1703484; d) J. Ran, T. Y. Ma, G. Gao, X.-W. Du, S. Z. Qiao, *Energy Environ. Sci.* **2015**, *8*, 3708-3717; e) S. Guo, Z. Deng, M. Li, B. Jiang, C. Tian, Q. Pan, H. Fu, *Angew. Chem. Int. Ed.* **2016**, *55*, 1830-1834; f) Y.-P. Zhu, T.-Z. Ren, Z.-Y. Yuan, *ACS Appl. Mater. Interfaces* **2015**, *7*, 16850-16856; g) Y. Zhang, T. Mori, J. Ye, M. Antonietti, *J. Am. Chem. Soc.* **2010**, *132*, 6294-6295.
- [27] G. Märkl, *Angew. Chem. Int. Ed.* **1966**, *5*, 846-847.
- [28] a) N. Hashimoto, R. Umamo, Y. Ochi, K. Shimahara, J. Nakamura, S. Mori, H. Ohta, Y. Watanabe, M. Hayashi, *J. Am. Chem. Soc.* **2018**, *140*, 2046-2049; b) C. Müller, D. Wasserberg, J. J. Weemers, E. A. Pidko, S. Hoffmann, M. Lutz, A. L. Spek, S. C. Meskers, R. A. Janssen, R. A. van Santen, *Chem. Eur. J.* **2007**, *13*, 4548-4559.
- [29] a) C. Müller, D. Vogt, *Comptes Rendus Chimie* **2010**, *13*, 1127-1143; b) H. Trauner, P. Le Floch, J.-M. Lefour, L. Ricard, F. Mathey, *Synthesis* **1995**, *1995*, 717-726; c) P. Le Floch, D. Carmichael, L. Ricard, F. Mathey, *J. Am. Chem. Soc.* **1993**, *115*, 10665-10670.
- [30] P. Tokarz, P. M. Zagórski, *Chem. Heterocycl. Compd.* **2017**, *53*, 858-860.
- [31] P. Kuhn, A. Forget, J. Hartmann, A. Thomas, M. Antonietti, *Adv. Mater.* **2009**, *21*, 897-901.
- [32] L. E. Broeckx, S. Güven, F. J. Heutz, M. Lutz, D. Vogt, C. Müller, *Chem. Eur. J.* **2013**, *19*, 13087-13098.
- [33] J. Hassan, M. Seignion, C. Gozzi, E. Schulz, M. Lemaire, *Chem. Rev.* **2002**, *102*, 1359-1470.
- [34] a) D. Schwarz, Y. S. Kochergin, A. Acharja, A. Ichangi, M. V. Opanasenko, J. Čejka, U. Lappan, P. Arki, J. He, J. Schmidt, *Chem. Eur. J.* **2017**, *23*, 13023-13027; b) T. D. Nelson, R. D. Crouch, *Organic Reactions* **2004**, *63*, 265-555; c) M. Alvaro, C. Aprile, B. Ferrer, H. Garcia, *J. Am. Chem. Soc.* **2007**, *129*, 5647-5655; d) M.-S. Kim, C. S. Phang, Y. K. Jeong, J. K. Park, *Polym. Chem.* **2017**, *8*, 5655-5659; e) D. Schwarz, Y. Noda, J. Klouda, K. Schwarzová - Pecková, J. Tarábek, J. Rybáček, J. Janoušek, F. Simon, M. V. Opanasenko, J. Čejka, *Adv. Mater.* **2017**, *29*, 1703399.
- [35] H. Kanter, W. Mach, K. Dimroth, *Eur. J. Inorg. Chem.* **1977**, *110*, 395-422.
- [36] J. Coates, *Encyclopedia of analytical chemistry* **2000**.
- [37] K. Dimroth, M. Lückoff, *Eur. J. Inorg. Chem.* **1980**, *113*, 3313-3317.
- [38] R. S. Sprick, B. Bonillo, M. Sachs, R. Clowes, J. R. Durrant, D. J. Adams, A. I. Cooper, *Chem. Commun.* **2016**, *52*, 10008-10011.
- [39] K. Dimroth, in *Phosphorus-Carbon Double Bonds*, Springer, **1973**, pp. 1-147.
- [40] K. Dimroth, W. Heide, *Chem. Ber.* **1981**, *114*, 3004-3018.
- [41] Z. Hu, A. P. Willard, R. J. Ono, C. W. Bielawski, P. J. Rossky, D. A. V. Bout, *Nat. Commun.* **2015**, *6*, 8246.
- [42] C. Yang, B. C. Ma, L. Zhang, S. Lin, S. Ghasimi, K. Landfester, K. A. Zhang, X. Wang, *Angew. Chem.* **2016**, *128*, 9348-9352.
- [43] K. Dimroth, W. Städe, *Angew. Chem. Int. Ed.* **1968**, *7*, 881-882.
- [44] A. Suzuki, *Angew. Chem. Int. Ed.* **2011**, *50*, 6722-6737.

**Phosphinine in  $\pi$ :** For the first time since its synthesis in 1966, the six-membered phosphinine ring is incorporated into a  $\pi$ -conjugated polymer. The phosphinine-based framework (CPF-1) has a high concentration of paramagnetic species, high thermal stability, green fluorescence and shows activity in photocatalytic splitting of water.



*Jieyang Huang, Ján Tarábek, Ranjit Kulkarni, Cui Wang, Martin Dračinský, Glen J. Smales, Yu Tian, Shijie Ren, Brian R. Pauw, Ute Resch-Genger, and Michael J. Bojdys\**

**Page No. – Page No.**

**A  $\pi$ -conjugated, covalent phosphinine framework**